

## On the plasmaphysics of plasma-etching

T.J. Bisschops, F.J. de Hoog

Physics Department, Eindhoven University of Technology,  
P.O.Box 513, 5600 MB Eindhoven, The Netherlands

**Abstract** - For the optimization of plasma-etching a basic knowledge of the plasma processes involved is often required. Considering the industrial etching needs and an understanding of the various etching mechanisms, the efforts of plasma research can be directed to the related plasma properties. Since there exist already numerous reactor types using vastly different plasmas as discussed in paragraph 1.3, a general discussion of the plasma physics involved is not possible. As topics the formation of sheath potentials in an RF discharge and the electron energy distribution of a  $CF_4$  plasma are more extensively discussed, since these dominate the ion fluxes. Diagnostics like mass spectroscopy, emission/absorption spectroscopy and electron density measurements lead to a better understanding of the plasma and may also serve industrial needs like e.g. end point detection.

### 1. INTRODUCTION

1.1. Studies on plasmas used for plasma-etching, in the end, always concentrate on the optimization of industrial processing techniques. Therefore, insight in the basic demands and mechanisms of plasma-etching is necessary to direct the efforts of plasma research. The ever decreasing lateral dimensions of integrated circuits necessitated the introduction of dry etching techniques. When the lateral dimensions are of the same order as the thickness of the layer to be patterned, anisotropic etching is needed. Though sputter etching (ion milling) with Argon could provide the desired anisotropy, problems concerning mask erosion, selectivity and etch rate were encountered. Using plasmas that produce chemically active species, through various mechanisms, the latter parameter can be increased; etch rates  $\geq 10^4$  Å/min have been obtained in  $SF_6-O_2$  plasmas [1]. When the etching of a layer has been completed, it is desirable that the underlying layer/substrate is not etched. To obtain the necessary selectivity in the etch process the discharge chemistry is altered, e.g. by an admixture of different gases; thus selectivity ratios  $\geq 50$  have been obtained [2]. For clarity the concepts of anisotropy and selectivity are depicted in figure 1.

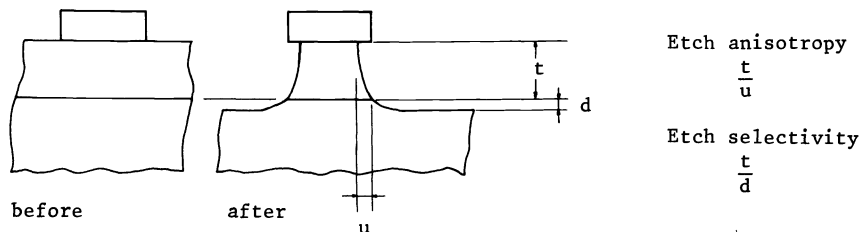


Figure 1 : Etch anisotropy and selectivity

The major drawbacks of wet etching, like the inability of etching small ( $< 3\mu m$ ) structures because of surface tension or gas bubble formation, its inherent isotropic etch nature and poor selectivity, can be overcome by dry etching. But also plasma etching has its drawbacks. The desired anisotropy and selectivity are not realised in every reactor type and often severe thermal loading of the wafer occurs. Problems concerning mask attack call for thick resist films and necessitate extra process-steps for resist hardening. Also some processes lead to substrate damage by high energy ion bombardment or residue formation.

1.2. In order to relate the desired etch characteristics to appropriate plasma properties a basic understanding of the actual etch mechanism is needed. Therefore three mechanisms will be briefly discussed and the influence of some plasma properties on the etching requirements concerning rate, anisotropy and selectivity will be given.

Closest to wet etching is the most simple mechanism : pure chemical etching, where no energetic particles are involved. It therefore is essentially isotropic and non-damaging. Since we are working in the gas phase the first step is chemisorption of active species (e.g. F). To achieve this, in many cases the chemisorption has to be dissociative. The next step is the formation of a reaction product (e.g.  $\text{Si} + 4\text{F} \rightarrow \text{SiF}_4$ ) which has to be volatile. The third step is the desorption of this reaction product. Molecular fluorine etches silicon spontaneously but with a very low etch rate. An increase of four orders of magnitude is achieved with  $\text{XeF}_2$  [3], in both cases the etching is proportional to the gas pressure, indicating that the first step (chemisorption) is limiting and that both the second and third step proceed at high rates. Studies of the chemisorption of halocarbons, that are frequently used in industry, show that dissociative chemisorption is not important [4]. Thus pure chemical etching is inhibited. From this it can be concluded that the gas discharge is needed to dissociate the inert halocarbons into fragments that readily react with silicon (e.g.  $\text{CF}_4$  to  $\text{CF}_3 + \text{CF}_3^+$ , [4, 5]). In this way the reactivity of fluorine can also be increased if first F-radicals are produced in a discharge [6].

The chemical etch rate can be drastically increased if the substrate is exposed to fluxes of energetic particles. Of far greater importance is ion bombardment of the substrate. But recently, especially in the area of maskless patterning, also electron beams and lasers are used to increase the etch rate. Concentrating on the ions a division can be made between ion enhanced chemical etching and chemically modified sputtering [7]. Depending on ion energy and chemical reaction volatilization ratio, either approach is more adequate. With the three process steps mentioned earlier as a guideline the effect of ions on chemical etching will be discussed briefly. Firstly the step of chemisorption can be modified in two ways. One is to transform non-active physisorbed species into fragments that show a great chemisorption rate by dissociation (e.g.  $\text{F}_2 \text{ ads} \rightarrow 2\text{F}$ ) [7]. The other way is by creating excited surface molecules which show a much higher reaction probability with the physisorbed species [8]. The product formation step can be altered by ion bombardment by means of thermally increasing the chemical reaction rate as is indicated by an Arrhenius plot or more drastically by breaking bonds which allow partially modified surface molecules to combine (e.g.  $\text{SiF}_2 \text{ surf} + \text{SiF}_2 \text{ surf} \rightarrow \text{Si} + \text{SiF}_4$  [9]). Also the third step, volatilization, can be modified. The desorption rate can be increased by the formation of volatile reaction products (see previous example), by increasing the surface temperature which leads to an increased sublimation rate or by increasing the desorbing surface area by surface roughening [10]. A quantitative description of various aspects of ion enhanced chemical etching is given in a paper by Gerlach Mayer [8].

Physical sputtering is a well known technique for the removal of surface layers, and is usually performed with  $\text{Ar}^+$ -ions. Also in the field of plasma etching sputtering can play a significant role. For the sake of selectivity and resist integrity again halogenated molecules are used. An article by Dieleman [11] deals with the various aspects of physical sputtering. Here only the sputtering of Si and  $\text{SiO}_2$  with  $\text{CF}_n^+$  ions and the concept of the modified surface film will be discussed. For ion energies in the range of 50...1000 eV the yield of  $\text{CF}_n$  species sputtering Si is less than for Ar. For  $\text{C}^+$  and  $\text{CF}^+$ , carbon deposition occurs at low energies which further lowers the sputtering rate. For  $\text{CF}_2^+$  and  $\text{CF}_3^+$  yields of 1 and 1.3 are obtained but these remain below yields expected from the shrapnel concept [12]. There is, so to say a chemical reduction in yield rather than enhancement. In a physical sputtering situation products leaving the surface are mostly  $\text{SiF}_2$  and  $\text{SiF}$ , in contrast with chemical etching where the main product is  $\text{SiF}_4$ . The concept of the modified surface film states that these products were initially present in the upper layer (10 Å) of the substrate. The products may have formed through chemisorption (which may be ion-enhanced) or recoil implantation. With the apparatus described in [11] the effects of chemical and physical etching can be separated. The experiments show that the neutral products have a low halogen ratio (e.g.  $\text{SiF}$ ,  $\text{SiF}_2$ ) and their cascade energy distribution indicates initial binding energies of  $\approx 0.2$  eV. The energy distribution further indicates that they left the substrate essentially by sputtering and not through thermal desorption. Relating these basic mechanisms with the desired etch properties e.g. anisotropy, selectivity and rate, shows that also the discharge chemistry is of importance and that the different properties are sometimes interrelated.

The etch rate depends on the abundance of chemical active species and on the intensity of ion bombardment. If any of these mechanisms is rate limiting also their ratio is of importance. With increasing ion energy the etch rate rapidly rises, but this may lead to sputter dominated etching which has low selectivity and also causes surface damage. The use of large fluxes of relatively low energetic ions (1-10 eV) seems therefore favourable. The etch rate is also strongly dependent on surface (reactor) temperature [13] which, without adequate substrate cooling may also introduce a time-dependent etch-rate. The abundance of chemical active species can not only be controlled by the discharge intensity but also by its chemistry. For example the admixture of oxygen to a  $\text{CF}_4$ -discharge, through various mechanisms [7], causes a net increase of free fluorine.

The major cause of anisotropic etching is bombardment by directionalized ions. This may be by stimulating chemisorption (surface damage), or by increasing the product formation

or desorption. Another mechanism is the formation of recombinants which prevent further etching of surfaces on which the ions are not incident. A comparison between the increased anisotropy by surface damage and the recombinant mechanism is given in litt.

[9] as a function of energy and pressure. If the etching is both of pure chemical and of ion stimulated nature, anisotropy can be increased by suppressing the chemical mechanism by changing the chemistry of the process. The degree of anisotropy is directly related to the directionality of the incident ions. If several collisions occur before the ion has passed the plasma sheaths (depending on  $E/p$ ) the directionality may be (partially) lost. A concept concerning this dependence on ion energy transport directionality is given by Zarowin [14].

The ratio of etch rates between several surface components (selectivity) is mostly influenced by changing the discharge chemistry using halogenated carbons, addition of hydrogen or oxygen changes the fluorine content in the discharge and allows for preferential etching of either  $\text{SiO}_2$  or Si [2, 3, 10]. Here also the volatilization of the carbon deposit on the surface plays an important role. As stated earlier, selectivity is decreased by sputter effects.

1.3. To obtain the desired chemical active species and ion bombardment numerous reactors have been developed. For isotropic etching the barrel reactor and plasma effluent reactors using RF or microwave excitation are used. In these reactors the lifetime of active species is very important and wall-interaction mechanisms can play a dominant role in the plasma chemistry. Most common is the parallel plate reactor, where the plasma is produced between planar electrodes or hexagonal electrodes. Here the plasma is in contact with the wafer and ion bombardment is used to increase the etch rate and to achieve anisotropy. Since the sheath potential depends on the electrode surface area ratio, a large potential (up to 2 kV) may be present in front of the smallest electrode, leading to reactive ion etching. To obtain optimal etch results plasma parameters are varied over a wide range : pressures from  $10^{-3}$  ... 10 torr and excitation frequencies either in the LF range (50...400 kHz) or RF (13.56 MHz). Different methods are used to increase the plasma intensity : producing extra electrons with auxiliary discharges or filaments (triode etching [15] ), by using magnetic fields to confine the electrons [16, 17], or by increasing the gas pressure and power density. The latter method has the disadvantage of losing ion directionality by collisions with neutrals in the sheath. Another approach is to use a separate plasma (e.g. microwave) for the production of active species and a second power source (RF) for sheath formation [18, 19]. A recent review article on different plasma processes used for plasma etching is given by Fonash [20] , discussing also the etching characteristics of the various methods.

## 2. DISCHARGE PHYSICS

2.1. Within the scope of this presentation we would like to present an overview of recent developments in the understanding of the physics of RF-discharges working at frequencies about 10 MHz. This of course limits the scope and represents a personal choice by the authors. Several important types of discharges applied in plasma chemistry will be omitted but the problems involved with the use of the planar RF-discharge appear to be typical for quite a number of applications of non-equilibrium, low density plasma devices for the processing of solid state interfaces.

Although consensus exists about the main features, until recently the details of the discharge physics involved appear to be somewhat underdeveloped. E.g. the subdivision of the planar discharge in a glow region and two sheaths regions is generally accepted and stands firmly on the basis of the Langmuir sheath model. However, the specific time dependence of charged particle fluxes towards the electrodes has not been measured in detail and consequently time dependent behaviour of sheath potentials is unclear. This has strong implications for the way power is absorbed in the discharge [21] and is important for etching applications, where etching is enhanced by energetic incoming ions. Beside considerations on the Langmuir model, where the particle current fluxes from the plasma towards the electrodes are central, the RF-discharge can be considered composed of a number of electrical circuit elements. Especially at higher frequencies where displacement currents become dominant, this model can be successful in interpreting etching results.

Another important feature is the electron energy distribution. In the last ten years model calculations of electron energy distributions have been increasingly focused from atomic gases towards molecular gases [22]. Strong impetus has been received from the modelling of molecular gas lasers. But the problems involved in RF-plasmas are not only more complicated by the varying electric fields but also by the electrode effects. This implies that spatial dependency should be taken into account [23]. An important question is whether energetic ions from the glow may cause secondary electron emission at the electrodes. Within the glow these accelerated electrons with energies comparable to the RF-amplitude may play an important role in the ionization-diffusion balance of the plasma [24].

## 2.2. SHEATH POTENTIALS

In an RF-driven planar discharge we can discern three regions. The glow region where a quasi-neutral plasma exists and the two boundary layers where space charges maintain a strong potential difference. Very often one sees this set up represented by the electrical network of fig. 2. The impedance of the glow is represented by  $R_g$ . The sheaths

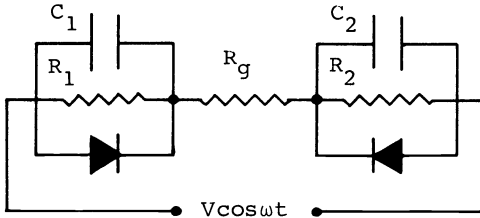


Fig. 2 : Equivalent network of RF-discharge

by the capacities  $C_1$  and  $C_2$  parallel to the leakage resistors  $R_1$  and  $R_2$  resp. The space charge in front of the electrodes is represented by the charge on the capacities and the leakage current of ions from the discharge seeps through  $R_1$  and  $R_2$ . The diodes are present because no plasma will be maintained against an electrode with higher potential. The glow will have positive potentials  $V_g - V_1$  and  $V_g - V_2$  with respect to electrode 1 and electrode 2 resp. In a stationary situation, because of the continuous leak of positive charge from the capacities, the diode parallel to the smallest capacity will during part of one RF-cycle charge the larger capacity to maintain the average values of the sheath potentials. The leakage rate determines how long the diode switch has to be open. If the leakage is negligible then the average value of the sheath potential is

$$V_g - V_2 = V_g - V_1 = C_2 / (C_1 + C_2) v,$$

where  $v$  is the RF-amplitude and  $C_2 \geq C_1$ .

This model has been successful in explaining a number of experimental observations. Assuming that the capacities are proportional to the electrode area, from the ratio of electrode areas, the sheath potentials can be estimated. E.g. in a recent paper Köhler et al [25] reported on measurements of bombardment energies of ions on the electrodes in an argon RF-discharge. The experiments in a D.C. and A.C. -coupled set up appear to sustain a linearized sheath model of the discharge. Zarowin et al [14] determined the relation between the etching anisotropy of polysilicon in a  $\text{CCl}_4$ -plasma and the power input. They used the model to relate the power input to the sheath potential which determines the anisotropy.

An equivalent circuit as in Fig. 2 cannot be a fully sound basis for analyzing all aspects of RF-discharge behaviour for all external parameter combinations. E.g. it does not explain all measurements of the glow potential in a A.C.-coupled situation as reported in ref.[25]. But more fundamentally, the representation of a space charge sheath by a capacity and the leakage of ion current by an ohmic resistor are only approximations. It is possible to acknowledge these non-linearities by the use of concepts from probe theory by Langmuir. Assume an RF-plasma to exist within a volume, where also two electrodes, with contact surfaces  $A_1$  and  $A_2$  are present. The potential differences between the plasma and the surfaces are again  $V_g - V_1$  and  $V_g - V_2$ . If one assumes that the potential differences are mainly across the sheaths (i.e.  $R_g \sim 0$ ) and the Langmuir assumptions are valid it follows that the currents in the electrode leads are

$$i_1 = A_1 (j_i - j_e \exp - e(V_g - V_1)/kT_e) + i_{\text{diel } 1}$$

$$i_2 = A_2 (j_i - j_e \exp - e(V_g - V_2)/kT_e) + i_{\text{diel } 2}$$

Because  $i_1 = -i_2$  and assuming  $i_{\text{diel } 1} \approx -i_{\text{diel } 2}$  it follows that

$$V_g = \ln \frac{j_e}{j_i} + \ln \left\{ \frac{A_1 \exp v_1 + A_2 \exp v_2}{A_1 + A_2} \right\}. \quad (2.1)$$

Note that potentials  $V$  have been reduced to  $v$  by dividing through  $kT_e/e$ , where  $T_e$  is the electron temperature of electrons leaving the plasma. The electron, resp. ion current densities at the sheath-glow boundary are  $j_e$  and  $j_i$ , the electrode areas are  $A_1$  and  $A_2$ . The result (2.1) is rather specific because it implies instantaneous charge conservation. In a D.C.-coupled situation when  $v_1 = 0$  and  $v_2 = v \cos \omega t$ , with  $v \gg 1$ , one can write in that case

$$v_g = v \cos \omega t + \ln(j_e/j_i) + \ln A_2/(A_1 + A_2) \quad 0 < \omega t < \pi/2$$

$$v_g = \ln(j_e/j_i) + \ln A_1/(A_1 + A_2) \quad 0 < \omega t < \pi \quad (2.2)$$

In fig. 3 one sees the development of  $v_g$  and  $v_2$  both related to  $v_1 = 0$ . The average value of the sheath potentials is

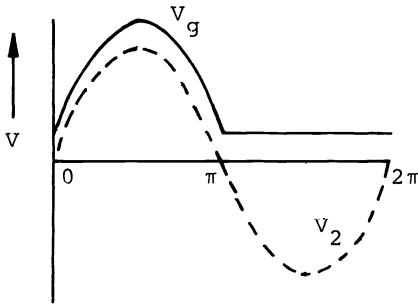


Fig. 3 : Potentials in a D.C.-coupled case ( $V_1 = 0$ )

$$\frac{v}{\pi} + \ln j_e/j_i + \ln A_2/(A_1 + A_2) . \quad (2.3)$$

If one assumes charge conservation to be effective only averaged over the RF-cycle it follows that this value is

$$\ln I_o(\frac{v}{2}) + \ln j_e/j_i ,$$

which can be approximated for large  $v$  by

$$\frac{v}{2} - \frac{\ln v}{2} + \ln j_e/j_i . \quad (2.4)$$

There are experimental indications that this dependency is confirmed [28]. However, the results of ref.[25] comply rather with the capacitance sheath model. In the A.C.-coupled case (see fig. 4 ) it is well known that the coupling capacitor gets a D.C. potential.

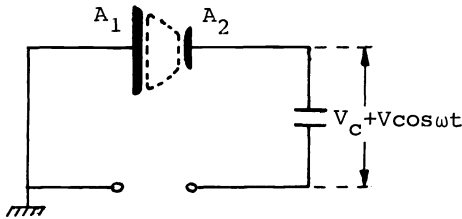


Fig. 4 : The A.C.-coupled case ( $V_1 = 0$ )

Here we will try to develop expressions for the value of this potential. Again assuming instantaneous charge conservation we may use (2.1). Neglecting the displacement currents we can write for the conduction current.

$$I_c = \frac{j_i}{2}(A_1 - A_2) \left\{ 1 - \frac{A_1 + A_2}{A_1 - A_2} \frac{A_1 \exp v_1 - A_2 \exp v_2}{A_1 \exp v_1 + A_2 \exp v_2} \right\} . \quad (2.5)$$

If we assume  $v_1 = 0$  and  $v_2 = v_c + v \cos \omega t$ , where  $v_c$  is the D.C. potential across the capacitor, we can develop an expression for  $v_c$  by requiring the current  $I_c$  through the system to have no D.C. component. Again for  $v_c \gg 1$  from (2.5) we find

$$v_c = v \cos \left\{ \frac{A_1}{A_1 + A_2} \pi \right\} + \ln \frac{A_1}{A_2}.$$

Note that the electrode will be negatively biased when  $A_1 > A_2$  and positive for  $A_2 > A_1$ . From the measurements by Köhler et al [25] we can see that their value of  $A_1/(A_1 + A_2)$  was .883 which is in accordance with the ratio of his electrode areas. Substituting  $v_2 = v_c + v \cos \omega t$  in (2.1) the expression for the value of  $v_g - v_1$  becomes

$$v(\cos \omega t - \cos \frac{A_2}{A_1 + A_2} \pi) + \ln j_e/j_i + \ln A_2/(A_1 + A_2)$$

$$0 < \omega t < A_2/(A_1 + A_2)\pi$$

$$\ln j_e/j_i + \ln A_2/(A_1 + A_2) \quad A_2/(A_1 + A_2)\pi < \omega t < \pi$$

If  $A_2$  is small the value of  $\overline{v_g - v_1}$  becomes also small and may approach  $\ln j_e/j_i$ .

Finally from the relations developed we can find the ratio between the average sheath potentials in the A.C.-coupled case. This is a very important relation as well as for sputter deposition as for etching applications. It appears that

$$\frac{v_g - v_1}{v_g - v_2} = \frac{\sin S_2 \pi - S_2 \pi \cos S_2 \pi + [\pi \ln (j_e/j_i) + \pi \ln S_1]/v}{\sin S_2 \pi + S_2 \pi \cos S_2 \pi + [\pi \ln (j_e/j_i) + \pi \ln S_1]/v}$$

where  $S_1 = A_1/(A_1 + A_2)$  and  $S_2 = A_2/(A_1 + A_2)$ .

Numerical calculations show that for relative large  $v$  this ratio scales with  $(A_1/A_2)^{-3}$ . An analysis by Horowitz [29] of sputtering plasma experiments appear to follow this dependency better than the  $(A_1/A_2)^{-4}$  dependency from the model by Koenig and Maisel [30].

So although successful in some respect it appears that the Langmuir model cannot explain all experimental data. But the capacitance sheath models also have their problems in explaining known data. Apparently to balance the electrode currents it is not necessary for the plasma to be short circuited against the electrodes during half of the cycle. But to consider the discharge as a semi-linear device described by circuit elements is also too simple.

Models should at least take into account dielectric currents in order to improve upon the Langmuir model. The convection currents e.g. are to be considered modulated by the past history of the ions and electrons in the sheath. But apart from theory there is a large shortage of consistent data on sheath potentials and a lot of work needs to be done.

### 2.3. ELECTRON ENERGY DISTRIBUTIONS

Electron energy distributions (EED) in RF-discharges are important in many respects. They define both the transport properties of the plasma and the production rates of ions, electrons and excited particles. An important parameter in the calculation of an EED is the product  $\omega \tau_m$ , where  $\omega$  is the RF frequency and  $\tau_m$  is the momentum transfer time for electron-molecule collisions. Is  $\omega \tau_m < 1$ , then in most gases the EED will be able, at least partly, to follow the field and will show modulation. Is  $\omega \tau_m > 1$ , then the EED is determined by stochastic heating.

Margenau [31] showed that in a homogeneous plasma, without electron-electron interactions and inelastic collisions a quasi-maxwellian distribution develops with an average energy

$$\langle \epsilon \rangle \approx M \frac{(eE_0)^2}{(m\omega)^2}. \quad (2.6)$$

To be useful in the modelling of etch and/or deposition plasmas this simple picture should be extended to include inelastic collisions, electron-electron interaction and spatial non-uniform effects. Up to now this program has been hardly executed. Solving the Boltzmann equation (BE) for the electrons including all these aspects presents a formidable task and only isolated aspects of the problem have been subject of study. In practical situations i.e. in planar RF-discharges at frequencies around 13,5 Mhz, pressures around 1 torr in molecular gas it occurs that  $\omega \propto 1/\tau_m$ , attachment, vibrational excitation are present and the distance between the electrodes is such that spatial effects should be taken into account.

To give more insight in the scaling of the average energy  $\langle \epsilon \rangle$  we follow a reasoning by Eletsii and coworkers [32]. Since in the case  $\omega \tau_m > 1$  the electron gains an amount of energy in the order of  $e^2 E_0^2 / (m\omega^2)$  between two consecutive elastic collisions,  $M/m$  collisions are necessary to get to average energy (2.6). But in a limited volume there is also a diffusion limited electron lifetime  $\tau_D$  dependent on the size of the container as well as on the ambipolar diffusion coefficient. If

$$v_m \tau_D < M/m$$

the average energy is given by

$$\langle \epsilon \rangle \approx \frac{(eE_0)^2}{m\omega^2} \frac{v_m}{v_D},$$

where  $v_m = \tau_m^{-1}$  and  $v_D = \tau_D^{-1}$ . In this case the average energy is less than that in expression (2.5) and scales with the square of the gas pressure. This reasoning can be extended to all inelastic processes defined by lifetimes  $\tau_{inj}$  ( $j = 1, 2, \dots$ ) when one can assume

$$v_m \tau_{in} < M/m.$$

The scaling yields in that case

$$\langle \epsilon \rangle \approx \frac{(eE_0)^2}{m\omega^2} v_m \sum_{j=1} \frac{1}{v_{inj}},$$

where  $v_{inj} = \tau_{inj}^{-1}$ .

When estimating these values for the situation defined, values of  $\langle \epsilon \rangle$  in the order of a few eV can be expected.

Solutions of the BE should however give final answers. Recently Winkler et al [33] calculated the time dependent of the first term in the spherical harmonic expansion, albeit only in the homogeneous situation in neon taking into account only elastic and excitation collisions. This term, representing the EED, was calculated for different frequencies  $\omega$ . For parts of the EED with energies below the excitation threshold, the energy loss rate is of the order  $m v_m / M$ .

So when

$$\omega > \frac{m}{M} v_m,$$

the low energy part of the EED cannot follow the modulation. The high energy part, where the energy loss rate is simply  $\sum v_{inj}$  cannot follow when

$$\omega > \sum_{i=1} v_{inj}.$$

So the bulk of the EED will at RF frequencies not follow the field modulation, but part of it can, depending on the field amplitude and the gas pressure. In our standard situation where e.g. vibrational processes play an important role,

$$\omega \tau_m \approx 1 \quad \text{and} \quad v_m \approx 10 \sum_{inj} v_{inj}$$

in first order no effects of field modulation in the EED can be expected.

An interesting point was made by Garscadden [24]. Starting from the idea that the electrodes in a planar reactor are bombarded by ions of 100 eV or more, he assumed that secondary electrons with a very high energy should be added to the BE as a source term at high energies. These electrons are very effective in carrying out inelastic collisions because of their energy but also because of confinement and multipactor effects. In this respect the influence of these electrons is similar to fast electrons in a hollow cathode glow discharge. This idea has been checked in a mixture of silane and hydrogen. Numerical calculations showed that the ratio of the number of fast electrons to the number of slow electrons could be  $10^{-4}$ .

Finally we would like to mention the work of Vallinga et al [23]. He actually solved the BE in the standard situation in a  $CF_4$  etching plasma ( $\omega = 8.5 \cdot 10^{-7} \text{ s}^{-1}$ , pressures about 0.5 torr, electrode distance about  $10^{-2} \text{ m}$ ). Here again  $\omega \tau_m \approx 1$ . Instead of a Fourier expansion in the time, a multiple time scale formalism was used. The approach included elastic collisions and excitation, ionization, dissociative attachment and vibrational excitation. The spatial dependency was also taken care of. From the particle balance it was possible to obtain expressions for the breakdown and steady state values of the effective field strength:

$$E_e = \frac{E_o}{\sqrt{1 + (\omega\tau_m)^2}}$$

The result of these calculations can be seen in Fig. 6. It appears that at high energies the distribution lies in between a Maxwellian and a Druyvesteyn distribution with the same average energies. At lower energies the distribution follows a Maxwellian. In Fig. 5 the breakdown ( $E_b$ ) and the maintenance values ( $E_m$ ) of the effective field strength in the glow are shown as a function of  $CF_4$ -pressure.

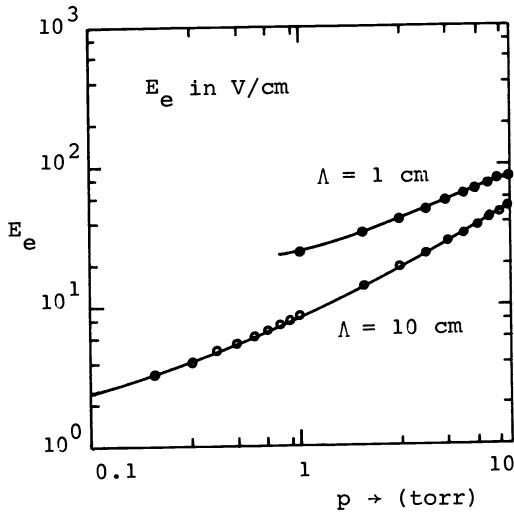


Fig. 5 : Breakdown and maintenance values of the electric field

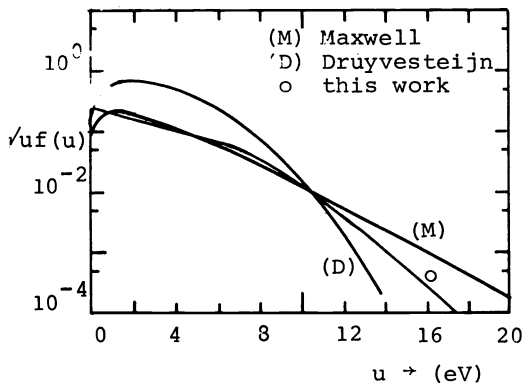


Fig. 6 : Electron energy distribution in  $CF_4$   
 $E_e/p = 12$  V/cm torr  
 $(\Lambda = 9.7$  cm)

### 3. EXPERIMENTAL METHODS

Experimental studies of etching plasmas use various diagnostics e.g. mass spectroscopy, optical diagnostics and electron density measurements.

#### 3.1. MASS SPECTROSCOPY AND OPTICAL DIAGNOSTICS

Mass spectroscopy is a very powerful and relative simple tool to study the discharge and reaction chemistry. It may be used in an effluent situation (sampling neutral products) or the mass spectrometer may be located in an electrode which also allows for the extraction of charged particles [33, 34, 35]. In the latter case not only the reactive neutrals or reaction products may be analyzed, but also the ions impinging in the surface. Using an energy analyzer it is possible to measure the ion energy distribution, which in some cases, can be directly related to the sheath potential [25]. Mass spectroscopy studies on negative ions are greatly complicated because negative ions can not readily leave the plasma, therefore afterglow techniques or beam extraction would be necessary.



Optical diagnostics like emission spectroscopy may also lead to considerable insight in the plasma density of the discharge [36]. Besides first identifying species and measuring their luminous intensity as a function of discharge parameters, also absolute densities can be inferred. If a known percentage of probe gas (e.g. Ar, N<sub>2</sub>) is mixed with the process gas relative intensities of e.g. F lines and Ar lines allow for a determination of absolute F densities. The applicability of this actinometric method is discussed in several papers by d'Agostino [37, 38] and Gottscho [39]. Absolute densities of molecular species e.g. SiF<sub>4</sub>, CO can be readily determined by infrared absorption spectroscopy [41]. For a 0.13 torr, 100 W CF<sub>4</sub> discharge these are in the range of 2.10<sup>20</sup> m<sup>-3</sup>.

A very powerful technique is L.I.F. which allows for spatially resolved density measurements which can also be time-resolved [41, 42, 43, 44].

3.3. ELECTRON DENSITIES

Since electrons play a dominant role in low-pressure, low-temperature plasmas, knowledge of the electron density and also electron temperature is essential for plasma modelling. Both parameters can be experimentally determined by probe measurements. Performing reliable probe measurements in RF plasmas is however very difficult, e.g. different authors give electron temperatures ranging from 2...14 eV or even as high as 30 eV.

Electron temperatures of 3.16 eV as calculated from measured plasma potentials [25] compare favourable with the values derived with the multiple time scale formalism discussed in section 2, see also [23]. Electron densities have been determined for low pressure (< 27 Pa). Low power density (0.1 W/cm<sup>2</sup>) plasmas with a microwave cut-off method [45], indicating densities in the 10<sup>15</sup> m<sup>-3</sup> range for Ar, O<sub>2</sub> and CHF<sub>3</sub>. Another method, developed by one of the authors, uses a single wafer etch reactor constructed as a microwave cavity [46]. Measuring the frequency shift of different resonant modes allows for electron density determination and also gives a rough spatial density distribution. Figure 7 shows the electron density in a CF<sub>4</sub> plasma as a function of pressure and power. In contrast to [45], electron densities measured in Ar are substantially (~ factor 10) higher, also no maximum is found.

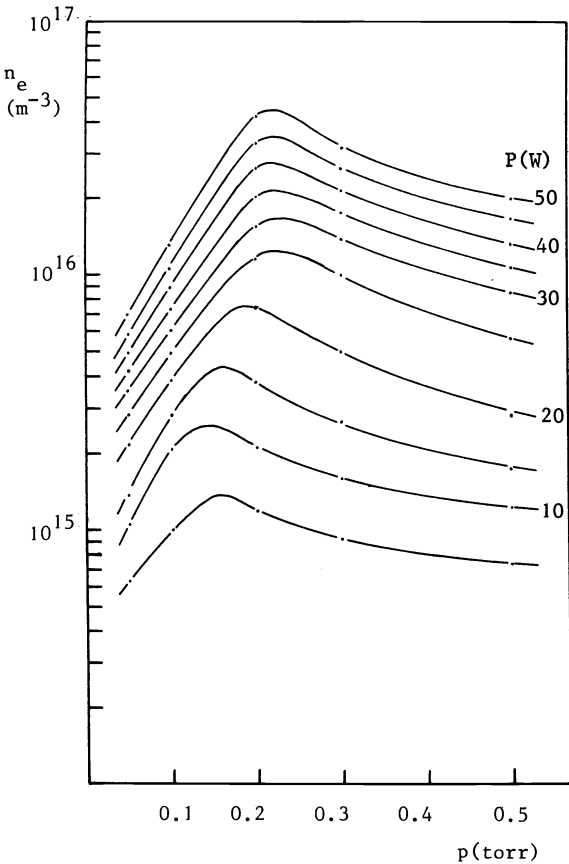


Fig. 7 : Electron density in CF<sub>4</sub> measured

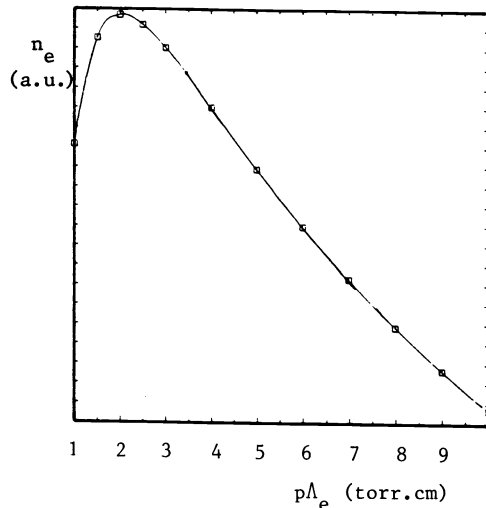


Fig. 8 : Electron density in CF<sub>4</sub> theory

Comparison with figure 8, showing electron densities as calculated with the multiple time scale formalism, indicates that the maximum in figure 7 is in perfect agreement with theory ( $\lambda_e = 10$  cm). Recent experiments, using an ellipsometer to determine the etch rate in situ [40] indicate that, at maximum  $n_e$ , also the etch rate shows a maximum.

#### Acknowledgement

The authors would like to acknowledge the support by the Netherlands Technology Foundation (S.T.W.).

#### References

- [1] R.C. d'Agostino, D.L. Flamm, J.Appl.Phys. 52(1), (1981), 162.
- [2] L.M. Eprath, Solid State Technology, July 1982, 87.
- [3] H.F. Winters, J.Appl.Phys. 49 (1978), 5165.
- [4] H.F. Winters, J.W. Coburn, Appl.Phys.Lett. 34 (1979), 70.
- [5] J.W. Coburn, H.F. Winters, T.J. Chuang, J.Appl.Phys. 48 (1977), 4973.
- [6] Chemical Dry Etching System CDE-IV Tokuda Seisakusho Ltd., Kawasaki, Japan.
- [7] J.W. Coburn, H.F. Winters, J.Vac.Sci.Technol. 16 (1979), 391.
- [8] U. Gerlach-Meyer, Surf.Science 103 (1981), 524.
- [9] D.L. Flamm, V.M. Donnelly, Plasma Chem.Plasma Proc. 1 (1981), 317.
- [10] V.M. Donnelly, D.L. Flamm, C.W. Tu, R.E. Ibbotson, to be published.
- [11] J. Dieleman. Le Vide - les Couches Minces, Supp. vol.218 (1983), 3.
- [12] P.C. Zalm, 10<sup>th</sup> Conf. on Atomic Coll. in Solids, July 1983.
- [13] R.G. Poulsen, J.Vac.Sci.Technol. 14 (1977), 266.
- [14] C.B. Zarowin, J.Vac.Sci.Technol. A2(4) (1984), 1537.
- [15] Solid State Technol., March 1984, 57.
- [16] Lin I, D.C. Hinson, W.H. Class, R.L. Sandstrom, Appl.Phys.Lett. 44(2) (1984), 185.
- [17] E.R. Lory, Solid State Technol. nov. 1984, 117.
- [18] Y. Arnal et al, Appl.Phys.Lett. 45(2) (1984), 132.
- [19] K. Suzuki, K. Ninomiya, S. Nishimatsu, Vacuum 34, 953.
- [20] S.J. Fonash, Solid State Technol. jan.1985, 150.
- [21] V.A. Godyak, Sov.Phys.Techn.Phys. 16 (1972), 1073.
- [22] M. Capitelli, C. Gorse, J. Wilhelm, R. Winkler, Annalen der Physik 41 (1984), 119.
- [23] P.M. Vallinga, T. Bisschops, H.T.C. Stoof, Proc. VII<sup>th</sup> Symp. Plasma Chemistry, Eindhoven, 1985.
- [24] A. Garscadden, Europhysics Conference Abstracts VII ESCAMPIG, Bari, vol.8E (1984), 16.
- [25] K. Köhler, J.W. Coburn, D.E. Horne, E. Kay, J.Appl.Phys. 57 (1985), 59.
- [26] C.B. Zarowin, R.S. Horvath, J.Electrochem.Soc. 129 (1982), 2541.
- [27] V.A. Godyak, A.A. Kuzovaikov Sov.J.Plasma Phys. 1 (1975), 276.
- [28] C.M. Horwitz, J.Vac.Sci.Techol. A1 (1983), 60.
- [29] H.R. Koenig, L.I. Maissel, IBM J.Res.Dev. 14 (1970), 168.
- [30] J.H. Margenau, Phys.Rev. 73 (1948), 297.
- [31] A.V. Evseev, A.V. Eletsii, High Temperature 19 (1981), 7.
- [32] R. Winkler, H. Deutsch, J. Wilhelm, Ch. Wilke, Beitr.Plasmaphysik 24 (1984), 285.
- [33] C.I. Beenhakker, R.P. v.d. Poll, J. Dieleman, Proc. 3<sup>rd</sup> Symp. Plasma Proc., 401.
- [34] H.J. Tiller, R. Göbel, U. Führ, Beitr.Plasmaphysik 24 (1984), 487.
- [35] K.E. Greenberg, J.T. Verdeyen, J.Appl.Phys. 57 (5), 1596.
- [36] D. Field, A.J. Hydes, D.F. Klemperer, Vacuum 34 (1984), 563.
- [37] R.C. d'Agostino et al, PlasmaChem.Plasma Proc. 4 (1984), 163.
- [38] R.C. d'Agostino et al, J.Appl.Phys. 54(3) (1983), 1284.
- [39] R.A. Gottscho, V.M. Donnelly, J.Appl.Phys. 56(2), (1984), 245.
- [40] T. Bisschops, G.M.W. Kroesen, Proc. VII<sup>th</sup> Symp. Plasma Chemistry, Eindhoven, 1985.
- [41] R.A. Gottscho et al, J.Appl.Phys. 55(7) (1984), 2707.
- [42] R.M. Roth, K.G. Spears, G. Wong, Appl.Phys.Lett. 45(1) (1984), 28.
- [43] L.F. di Mauro, R.A. Gottscho, T.A. Miller, J.Appl.Phys. 56(7) (1984), 2007.
- [44] R. Walkup et al, Appl.Phys.Lett. 45(4) (1984), 372.
- [45] C.A.M. de Vries, A.J. van Roosmalen, G.C. Puylaert, to be published.
- [46] T. Bisschops, H. Störi, Proc. VII<sup>th</sup> Symp. Plasma Chemistry, Eindhoven, 1985.